Neurochemistry International 81 (2015) 41–47

Contents lists available at ScienceDirect

Neurochemistry International

journal homepage: www.elsevier.com/locate/nci

The effects of JM-20 on the glutamatergic system in synaptic vesicles, synaptosomes and neural cells cultured from rat brain

Yanier Nuñez-Figueredo [a], Gilberto L. Pardo Andreu [b,*], Samanta Oliveira Loureiro [c], Marcelo Ganzella [c], Jeney Ramírez-Sánchez [a], Estael Ochoa-Rodríguez [d], Yamila Verdecia-Reyes [d], René Delgado-Hernández [a], Diogo O. Souza [c,**]

[a] Centro de Investigación y Desarrollo de Medicamentos, Ave 26, No. 1605 Boyeros y Puentes Grandes, CP 10600, Ciudad Habana, Cuba
[b] Centro de Estudio para las Investigaciones y Evaluaciones Biológicas, Instituto de Farmacia y Alimentos, Universidad de La Habana, ave. 23 # 21425 e/214 y 222, La Coronela, La Lisa, CP 13600, Ciudad Habana, Cuba
[c] Departamento de Bioquímica, PPG em Bioquímica, Instituto de Ciências Básicas da Saúde, Universidade Federal do Rio Grande do Sul, Rua Ramiro Barcelos, 2600 anexo, Porto Alegre, RS 90035-003, Brazil
[d] Laboratorio de Síntesis Orgánica de La Facultad de Química de La Universidad de La Habana (Zapata s/n entre G y Carlitos Aguirre, Vedado Plaza de la Revolución, CP 10400, Ciudad de la Habana, Cuba

ARTICLE INFO

Article history:
Received 1 October 2014
Received in revised form 24 December 2014
Accepted 15 January 2015
Available online 21 January 2015

Keywords:
JM-20
Glutamatergic system
Synaptic vesicle
Synaptosomes
Astrocytes
Neurons

ABSTRACT

JM-20 (3-ethoxycarbonyl-2-methyl-4-(2-nitrophenyl)-4,11-dihydro-1H-pyrido[2,3-b][1,5]benzodiazepine) is a novel benzodiazepine dihydropyridine hybrid molecule, which has been shown to be a neuroprotective agent in brain disorders involving glutamate receptors. However, the effect of JM-20 on the functionality of the glutamatergic system has not been investigated. In this study, by using different *in vitro* preparations, we investigated the effects of JM-20 on (*i*) rat brain synaptic vesicles (L-[^{3}H]-glutamate uptake, proton gradient built-up and bafilomycin-sensitive H^+-ATPase activity), (*ii*) rat brain synaptosomes (glutamate release) and (*iii*) primary cultures of rat cortical neurons, astrocytes and astrocyte–neuron co-cultures (L-[^{3}H]-glutamate uptake and glutamate release). We observed here that JM-20 impairs H^+-ATPase activity and consequently reduces vesicular glutamate uptake. This molecule also inhibits glutamate release from brain synaptosomes and markedly increases glutamate uptake in astrocytes alone, and co-cultured neurons and astrocytes. The impairment of vesicular glutamate uptake by inhibition of the H^+-ATPase caused by JM-20 could decrease the amount of the transmitter stored in synaptic vesicles, increase the cytosolic levels of glutamate, and will thus down-regulate neurotransmitter release. Together, these results contribute to explain the anti-excitotoxic effect of JM-20 and its strong neuroprotective effect observed in different *in vitro* and *in vivo* models of brain ischemia.

1. Introduction

In addition to being a physiologically important excitatory neurotransmitter, glutamate plays a pivotal role in various neurological disorders including cerebral ischemia. Its levels are increased during cerebral ischemia with excessive neurological stimulation resulting in glutamate-induced neuronal toxicity, known as excitotoxicity, and thus is considered the triggering spark in ischemic neuronal damage (Mehta et al., 2013; Nishizawa, 2001).

Glutamate transmission involves its accumulation into secretory vesicles and their subsequent exocytosis to the extracellular space (Lin and Scheller, 2000). The accumulation of glutamate in secretory vesicles is mediated by vesicular glutamate transporters (VGLUTs) (Juge et al., 2010). This process is driven by an electrochemical H^+ gradient (ΔpH) established by the vacuolar-type ATPases (V-ATPase) (Maycox et al., 1988; Naito and Ueda, 1985; Nelson and

Abbreviations: VGLUTs, vesicular glutamate transporters; V-ATPase, vacuolar-type ATPases; JM-20, 3-ethoxycarbonyl-2-methyl-4-(2-nitrophenyl)-4,11-dihydro-1H-pyrido[2,3-b][1,5]benzodiazepine; F-ATPase, mitochondrial F-type ATPase; DMEM, Dulbecco's Modified Eagle's Medium; DMSO, dimethyl sulfoxide; EGTA, ethylene glycol-bis(2-aminoethylether)-N,N,N′,N′-tetra acetic acid; DIV, days *in vitro*; GFAP, glial fibrillary acidic protein; ΔpH, vesicular transmembrane proton gradient; $F_{(i)}$, initial fluorescence intensity; $F_{(MgCl2)}$, fluorescence intensities after the addition of $MgCl_2$;; $F_{(0)}$, fluorescence intensities after the addition of Triton X-100;; Pi, inorganic phosphate; HBSS, Hank's Balanced Salt Solution; HPLC, high-performance liquid chromatography; AMPA, α-amino-3-hydroxy-5-methyl-4-isoxazolone-proprionic acid; NMDA, N-methyl-D-aspartate; EAATs, Na^+-dependent glutamate transporters.

* Corresponding author. Centro de Estudio para las Investigaciones y Evaluaciones Biológicas, Instituto de Farmacia y Alimentos, Universidad de La Habana, CP 13600, Ciudad Habana, Cuba. Tel.: (53) 7 2718534; fax: (53) 7 2603894.
E-mail address: gpardo@ifal.uh.cu (G.L. Pardo Andreu).
** Corresponding author. Departamento de Bioquímica, PPG em Bioquímica, Instituto de Ciências Básicas da Saúde, Universidade Federal do Rio Grande do Sul, Porto Alegre, RS 90035-003, Brazil. Tel.: (51) 33085558; fax: (51) 33085540.
E-mail address: diogo@ufrgs.br (D.O. Souza).

http://dx.doi.org/10.1016/j.neuint.2015.01.006
0197-0186/

Harvey, 1999). It is expected that both the electrochemical driving force and VGLUT activity affect vesicular glutamate content and subsequent glutamatergic signaling and release (Juge et al., 2010). We have recently observed that JM-20 (3-ethoxycarbonyl-2-methyl-4-(2-nitrophenyl)-4,11-dihydro-1H-pyrido[2,3-b][1,5]benzodiazepine) given 1 h after reperfusion at the neuroprotective dose of 8 mg/kg significantly reduced the glutamate concentration in cerebrospinal fluid from rats subjected to 90 min middle cerebral artery occlusion, compared with vehicle-treated rats (5.5 ± 1.55 μM versus 14.4 ± 3.48 μM) (Nuñez-Figueredo et al., 2014b). The glutamate levels in JM-20-treated rats were equivalent to normal values because no difference was observed when compared to those from a sham-operated group (4.5 ± 1.2 μM). Additionally, we identified the ability of this molecule to selectively inhibit the hydrolytic activity of mitochondrial F_1F_O ATP synthase at very low micromolar concentrations (IC_{50} = 5 μM) (Nuñez-Figueredo et al., 2014a). Because V-ATPase and mitochondrial F-type ATPase (F-ATPase) have a similar structure and mechanism of action (Nelson and Harvey, 1999), we hypothesized that the *in vivo* anti-excitotoxic effect of JM-20 observed elsewhere could be mediated by the inhibition of V-ATPase activity and the subsequent reduction in quantum release of glutamate into the synaptic cleft. To prove this hypothesis we evaluated the *in vitro* effects of JM-20 on the following preparations: (*i*) rat brain synaptic vesicles (L-[^{3}H]-glutamate uptake, proton gradient built-up, and V-ATPase activity), (*ii*) rat brain synaptosomes (glutamate release) and (*iii*) primary cultures of rat astrocytes, neurons and astrocyte–neuron co-cultures (L-[^{3}H] glutamate uptake and glutamate release).

2. Materials and methods

2.1. Compounds and reagents

All chemicals used were of the highest grade available and purchased from Sigma-Aldrich (St. Louis, MO, USA) unless otherwise specified. Fetal bovine serum (FBS), Dulbecco's Modified Eagle's Medium: Nutrient Mixture F-12 (DMEM), fungizone and penicillin/streptomycin were purchased from Gibco BRL (Carlsbad, CA, USA). Stock solutions of JM-20 were prepared daily in dimethyl sulfoxide (DMSO) and added to the cells in culture, synaptosomes or synaptic vesicles in reaction media at a 1/1000 (v/v) dilution, respectively. Control experiments contained DMSO at a 1/1000 dilution. JM-20 was synthesized, purified and characterized as previously reported (Figueredo et al., 2013).

2.2. Experimental animals

Male Wistar rats (3 months, 200–250 g) maintained on a 12 h light: 12 h dark schedule at 25 °C, with food and water ad libitum, were obtained from our local breeding colony. The experimental protocol followed the "Principles of Laboratory Animal Care" (NIH publication 85-23, revised 1985) and was approved by the Ethics Committee for Animal Research of the Federal University of Rio Grande do Sul.

2.3. Preparation of synaptic vesicles, synaptosomes, submitochondrial particles and cell cultures from rat brain

2.3.1. Synaptic vesicles

Synaptic vesicles were isolated from rat brains as previously described (Porciuncula et al., 2003). Briefly, crude synaptosomal fractions (P2) were obtained and osmotically lysed by resuspension (0.8 ml/g fresh tissue) in 10 mM Mops–Tris (pH 7.4) containing 0.1 mM ethylene glycol-bis(2-aminoethylether)-N,N,N′,N′-tetra acetic acid (EGTA) for 30 min and centrifuged at 32,800 *g* for 20 min. The pellet was considered as synaptosomal pellet in order to evaluate further the quality of synaptic vesicle fraction. The supernatant containing synaptic vesicles was subjected to 0.4 and 0.6 M sucrose density gradient centrifugation at 65,000 *g* for 2 h. The synaptic vesicle fraction was isolated from the 0.4 M sucrose band and stored at –70 °C.

2.3.2. Synaptosomes

The forebrain from male Wistar rats (3–4 months old) was rapidly removed and homogenized in isolation buffer containing 0.32 M sucrose, 1 mM EDTA (K^+ salt), and 10 mM Tris–HCl (pH 7.4). The homogenate was centrifuged at 1330 *g* for 3 min. The supernatant was carefully retained and then centrifuged at 21,200 *g* for 10 min. The pellet was resuspended and carefully layered on top of a discontinuous Percoll gradient and centrifuged for 5 min at 30,700 *g* (Sims, 1990).

2.3.3. Submitochondrial particles

Rat brain mitochondria were obtained using a discontinuous Percoll gradient protocol (Sims, 1990). The mitochondrial respiratory control ratio (state 3/state 4 respiratory rate ratio) was over 5, measured using 5 mM glutamate and 5 mM malate as NADH-linked substrates. Submitochondrial particles were obtained by freezing and thawing (three cycles) isolated mitochondria (20 mg/ml) as previously described for rat heart mitoplast (Uyemura and Curti, 1992).

Each preparation (synaptic vesicles, synaptosomes or mitochondria) was obtained from two whole rat brains. The protein concentration was determined using the method described by Lowry et al. (1951) with bovine serum albumin as a standard.

The quality of preparations (synaptosomes, and synaptic vesicles) was evaluated by western blotting, analyzing the immunocontent of the following proteins: synaptosomal-associated protein 25 (SNAP 25), vesicular glutamate transporter 2 (VGLUT), synaptobrevin (VAMP), synaptophysin, and vacuolar H^+ ATPases (V-ATPase) for synaptic vesicles; excitatory amino acid transporter 1 (GLAST), and excitatory amino acid transporter 2 (GLT-1), for astrocyte membranes; excitatory amino acid transporter 3 (EAAC1), N-methyl-D-aspartate receptor subunit NR1 (NR1), and postsynaptic density protein 95 (PSD95) for neuronal plasma membrane; and monoamine oxidase A (MAO A) and succinate dehydrogenase (SDH) for outer and inner mitochondrial membrane, respectively. High immunocontent of synaptic vesicle proteins with minimal or/no contamination of other cellular compartments in the synaptic vesicle preparations was obtained, compared to lysed synaptosomes pellets.

2.3.4. Cell cultures

Primary astrocyte cultures were prepared from the cerebral cortex of newborn (0–1-day old; P0) Wistar rats, as described previously (Loureiro et al., 2010). Briefly, rats were decapitated, brain structures were removed and the meninges were carefully stripped off. Cells were mechanically dissociated and plated in Dulbecco's modified Eagle's medium (DMEM) containing 10% fetal bovine serum (pH 7.4) supplemented with glucose (33 mM), glutamine (2 mM), and sodium bicarbonate (3 mM) into a 15.6 diameter well (24-well plate) that had been coated with polyornithine (1.5 mg/ml, Sigma, St. Louis, MO). Astrocyte cultures were maintained in an incubator at 37 °C in a humidified atmosphere of 95% air and 5% CO_2. Cultures were used at 15–20 days *in vitro* (DIV) with astrocytes showing a confluent monolayer consisting of >95% of glial fibrillary acidic protein (GFAP)-positive cells.

Primary neuronal cell cultures were prepared from the cerebral cortices of embryonic day 18 Wistar rats, as previously described (Moura Neto et al., 1983). Approximately 5×10^4 cells were plated on monolayer carpets of astrocytes for co-culture assays. Neurons and co-cultures were maintained *in vitro* for 7 days before being used in experiments.

2.4. Glutamate uptake

2.4.1. Vesicular glutamate uptake

Vesicular L-[^{3}H] glutamate uptake was performed in a standard medium (final volume of 200 µl) consisting of 10 mM Mops–Tris, pH 7.4, 4 mM KCl, 140 mM potassium gluconate, 0.12 M sucrose, 2 mM $MgCl_2$, and 2 mM ATP. Glutamate uptake was determined with 50 µM L-[^{3}H] glutamate (Amersham International). Specific uptake was calculated by discounting the uptake measured in the absence of ATP. Radioactivity was measured with a Wallac Model 1409 liquid scintillation counter (PerkinElmer-Wallac, Inc., Gaithersburg, Md). JM-20 was added at final concentrations of 0.1, 1, and 10 µM, based on previous results (Nuñez-Figueredo et al., 2014a).

2.4.2. Cell culture glutamate uptake

Cell cultures (astrocytes, neurons and co-cultures) were incubated for 15 min with an HBSS solution containing (mM): 137 NaCl, 0.63 Na_2HPO_4, 4.17 $NaHCO_3$, 5.36 KCl, 0.44 KH_2PO_4, 1.26 $CaCl_2$, 0.41 $MgSO_4$, 0.49 $MgCl_2$ and 5.55 glucose, adjusted to pH 7.4. [^{3}H] glutamate uptake was performed according to Frizzo et al. (2001) with some modifications. Briefly, uptake was carried out at 35 °C by adding 100 µM unlabeled glutamate and 0.33 µCi/ml L-[^{3}H] glutamate for 5 min. JM-20 (1 and 10 µM) was added 20 min prior to the addition of L-[^{3}H] glutamate. The reaction was terminated by two washes of ice-cold HBSS (4 °C) immediately followed by the addition of 0.5 N NaOH. Sodium-independent uptake was determined at 35 °C using HBSS containing N-methyl-D glutamine instead of NaCl and Na_2HPO_4. Sodium-dependent uptake was obtained by subtracting sodium-independent from total uptake. Incorporated radioactivity was determined with a Packard scintillator (TRI CARB 2100 TR). All experiments were performed in triplicate.

2.5. Vesicular transmembrane proton gradient (ΔpH)

ΔpH was determined by measuring the fluorescence quenching of acridine orange (1.5 µM) in a Spectra Max M5 microplate reader spectrophotometer as previously described using an excitation wavelength of 492 nm and an emission wavelength of 537 nm (Goh et al., 2011). The reaction was initiated by the addition of 1 mM $MgCl_2$ in the presence of 1 mM ATP to a reaction medium containing 30 µg of synaptic vesicle protein, 140 mM KCl, and 10 mM Mops–Tris (pH 7.4). The reaction was terminated by the addition of Triton X-100 to a final concentration of 10 µM. JM-20 effects were evaluated at 0.1, 1 and 10 µM. The percentage of fractional quench is calculated according to the following equation: % Fractional quench = $[F_{(i)} - F_{(MgCl2)}]/F_{(0)} \times 100$, where $F_{(i)}$ is the initial fluorescence intensity, and $F_{(MgCl2)}$ and $F_{(0)}$ are the fluorescence intensities after the addition of $MgCl_2$ and the dissipating detergent, respectively.

2.6. Measurement of V-ATPase and F_1F_0 ATPase activities

The activities of V-type ATPase (bafilomycin-sensitive H^+-ATPase activity) and F_1F_0 ATPase (oligomycin-sensitive ATPase activity) were measured in the media used for uptake experiments. Synaptic vesicles or submitochondrial particles (20 µg proteins) were pre-incubated for 10 min in the presence of 1 µM bafilomycin A1 (for vesicles) or 3 µM oligomycin (for submitochondrial particles) (Sigma, St. Louis, MO) with or without JM-20 (0.1, 1, and 10 µM) for 10 min at 35 °C. The incubation was stopped by the addition of 10% trichloroacetic acid (v/v). Samples were chilled on ice for 10 min, and 100 µl aliquots were withdrawn for assaying the released inorganic phosphate (Pi) as previously described (Chan et al., 1986), using malachite green as the color reagent. Controls where the synaptic vesicle or submitochondrial particle preparations were added after trichloroacetic acid were used for correcting non-enzymatic Pi release. The specific V-ATPase or F_1F_0 ATPase activities were calculated by subtracting the total ATPase activities (in the absence of bafilomycin or oligomycin) from the ATPase activity measured in the presence of such inhibitors.

2.7. Glutamate release in rat brain synaptosomes

Synaptosomes (250 µg) were incubated for 1 min with KCl at low (10 mM) or high (56 mM) concentrations in modified Hank's Balanced Salt Solution (HBSS) at 37 °C in the presence of JM-20 (1, 5 and 10 µM). For basal glutamate release, the synaptosomes were incubated in low-non depolarizing KCl (1.2 mM) HBSS. After, synaptosomes were centrifuged for 10 min at 14,000 *g*. Supernatants (25 µl) were used for glutamate determination by high-performance liquid chromatography (HPLC).

2.8. Glutamate determination by HPLC

The supernatants were derivatized with *o*-phthalaldehyde and separation was carried out with a reverse phase column (Supelcosil LC-18, 250 mm × 4.6 mm, Supelco) in a Shimadzu Instruments liquid chromatograph (50 µl loop valve injection). The mobile phase flowed at a rate of 1.4 ml/min and column temperature was 24 °C. Buffer compositions were as follows: buffer A: 40 mM $NaH_2PO_4 \times H_2O$ buffer, pH 5.5, containing 20% methanol; buffer B: 10 mM $NaH_2PO_4 \times H_2O$ buffer, pH 5.5, containing 80% methanol. The gradient profile was modified according to the content of buffer B in the mobile phase: 0% at 0.00 min, 25% at 13.75 min, 100% at 15.00–20.00 min, 0% at 20.01–25.00 min. Absorbance was read using 360 nm and 455 nm, excitation and emission, respectively, with a Shimadzu fluorescence detector. Samples of 50 µl were used and concentration was expressed in µM (Joseph and Marsden, 1986; Schmidt et al., 2009).

2.9. Statistical analysis

The software GraphPad Prism 5.0 (GraphPad Software Inc., USA) was used for statistical analysis. The data were expressed as the mean ± SEM. Comparisons between different groups were performed using one-way analysis of variance (ANOVA) followed by the Newman–Keuls multiple comparison test. Differences were considered statistically significant at $P < 0.05$.

3. Results

3.1. JM-20 specifically inhibits Bafilomycin-sensitive H^+-ATPase and the hydrolytic activity of F_1F_0ATPase in synaptic vesicles and brain submitochondrial particles, respectively

In our previous study, we showed that JM-20 inhibits the hydrolytic activity of F_1F_O-ATP synthase in mitochondria and submitochondrial particles isolated from rat liver (Nuñez-Figueredo et al., 2014a). Considering that F-ATPases and V-ATPases have structural and functional similarities, we hypothesized that this molecule may inhibit V-ATPase activity. Fig. 1 A and B shows that JM-20 inhibited the hydrolytic activity of brain mitochondrial F_1F_O-ATP synthase and vesicular H^+-ATPase activity, in a concentration dependent manner.

3.2. JM-20 prevents the formation of the vesicular ΔpH gradient

In nerve terminals, V-ATPase generates an electrochemical proton gradient (ΔpH) that is used by specific neurotransmitter-proton antiporters to accumulate neurotransmitters inside storage organelles. Seeing that JM-20 inhibited the activity of vesicular H^+-ATPase, we investigated the effects of this molecule on the vesicular ΔpH formation. Fig. 2Ashows that 0.1–10 µM JM-20 dissipated the ΔpH gradient formation of synaptic vesicles in a dose dependent

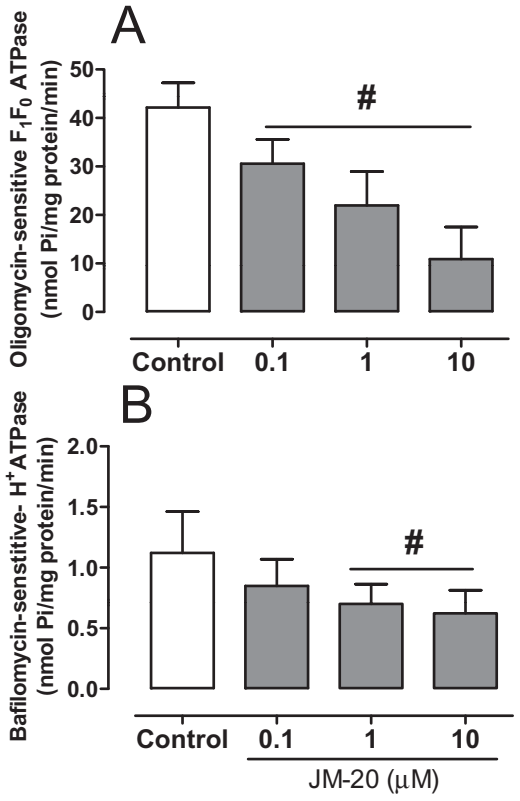

Fig. 1. Effect of JM-20 (0.1, 1, and 10 μM) or DMSO at 1/1000 v/v dilution (Control) on the hydrolytic activity of mitochondrial F_1F_O ATPase (A), and bafilomycin-sensitive H^+-ATPase activity (B). The results are expressed as the means ± S.E.M. of 3 independent experiments performed using different vesicle or submitochondrial particle preparations. The results were statistically analyzed using Student's *t* test. Statistically significant differences from controls are represented by # $p < 0.05$.

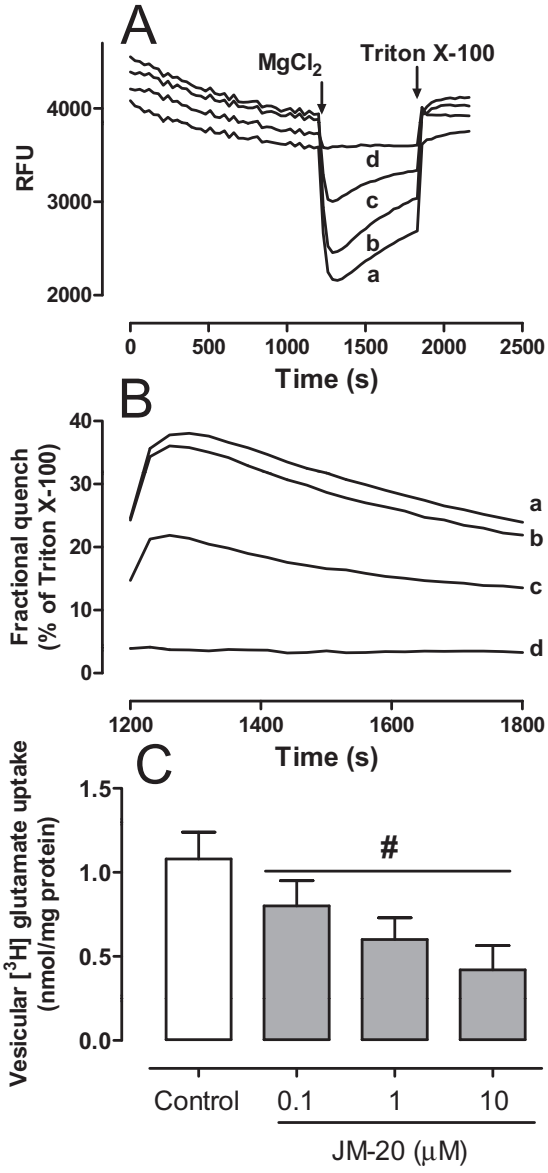

Fig. 2. Effects of JM-20 on synaptic vesicles and vesicular electrochemical proton gradient (ΔpH) formation. The reaction was initiated by the addition of 1 mM $MgCl_2$ (in the presence of 1 mM ATP), and terminated by the addition of Triton X-100 (10 μM) (A). The percentage of fractional quench is calculated according to the following equation: % Fractional quench = $[F_{(i)} - F_{(MgCl2)}]/F_{(0)} \times 100$, where $F_{(i)}$ is the initial fluorescence intensity, and $F_{(MgCl2)}$ and $F_{(0)}$ are the fluorescence intensities after the addition of $MgCl_2$ and the dissipating detergent, respectively. The conditions were: (a) Control (DMSO 1/1000 dilution), (b) JM-20 at 0.1 μM, (c) JM-20 at 1 μM, and (d) JM-20 at 10 μM. Traces are representative of three independent vesicular preparations (B). Effects of JM-20 (0.1, 1, 10 μM) on glutamate uptake by synaptic vesicles. Synaptic vesicles were incubated for 10 min with JM-20. The results are expressed as the means ± S.E.M. of 3 independent vesicle preparations. The results were statistically analyzed using Student's t test. Statistically significant differences from controls are represented by $^{\#}p < 0.05$ (C).

manner. This process was triggered by the addition of 1 mM $MgCl_2$ in the presence of 1 mM ATP and was terminated by the addition of 10 μM Triton X-100. The percentage of fractional quench (Fig. 2B) shows that JM-20 at 10 μM completely inhibited the formation of the proton gradient across vesicular membranes.

3.3. JM-20 inhibits glutamate uptake by synaptic vesicles

Considering that the vesicular glutamate uptake depends on ΔpH generated by the H^+-ATPase, we investigated the effects of JM-20 on glutamate uptake in synaptic vesicles. Fig. 2C shows that JM-20 inhibits specific L-[^{3}H]-glutamate uptake compared with control-treated synaptic vesicles in a concentration-dependent manner. The non-specific glutamate uptake (in the absence of ATP) was not affected by JM-20 (data not shown).

3.4. JM-20 inhibits glutamate release in rat brain synaptosomes

Inhibition of V-ATPase activity and consequent reduction of ΔpH elicited by JM-20 should decrease the amount of transmitter stored in synaptic vesicles and thus down-regulate transmitter release. Fig. 3shows that JM-20 dose dependently and in the low nanomolar range inhibited glutamate release ($P < 0.05$) by synaptosomes evoked by high (Panel A_56 mM) or low (Panel B_10 mM) KCl concentrations. Stimulating synaptosomes with low concentrations of KCl appears to uncover additional mechanism of release inhibition, which is dependent on Na^+ or K^+-channel-driven depolarization (Godino et al., 2007). The similar pattern of glutamate release inhibition observed at both depolarizing conditions suggests that JM-20 acts mainly on vesicular glutamate release (Ca^{2+}-dependent). Furthermore, this molecule did not interfere with the neurotransmitter release under basal non-depolarizing condition (result not shown).

3.5. JM-20 affected glutamate uptake in astrocytes and astrocyte–neuron co-cultures but not in neurons cultures

Astrocytes protect neurons through multiple mechanisms, including regulation of ionic homeostasis, control of extracellular

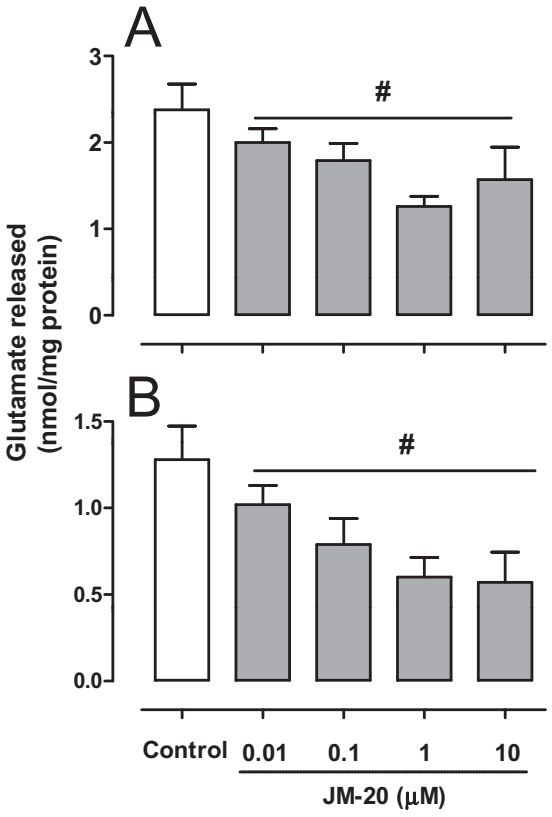

Fig. 3. Effects of JM-20 (1, 5, and 10 μM) on synaptosomal glutamate. Synaptosomes were incubated for 1 minute with high (56 mM) (A), or low (10 mM) KCl (B) in HBSS at 37 °C in the absence (Control) or presence of JM-20 (1, 5 and 10 μM). After incubation, synaptosomes were centrifuged for 10 min at 14,000 *g*. Supernatants (25 μl) were used for glutamate determination by high-performance liquid chromatography (HPLC). The results are expressed as the means ± S.E.M. of 3 independent vesicle preparations. Statistically significant differences from controls are represented by $^{\#}p < 0.05$ according to ANOVA and *post hoc* Newman–Keuls tests.

glutamate levels, and upregulation of glycolytic capacity during ischemia (Dienel and Hertz, 2005). In our experimental conditions, JM-20 did not stimulate glutamate uptake in neurons (Fig. 4B) but increased it in cultured astrocytes (Fig. 4A) at very low micromolar concentrations (0.01–1 μM). A strong tendency to increase the neurotransmitter uptake by JM-20 was also observed in neurons–astrocytes co-culture, being statistically significant at 1 μM. (Fig. 4C). Under the same experimental conditions, JM-20 (0.01, 0.1, 1 and 10 μM) did not induce glutamate release in any of the independent cultures used (Fig. 4D–F).

4. Discussion

Glutamate is a major excitatory neurotransmitter working at a variety of excitatory synapses in the nervous system. Pharmacological studies in rodents and recent clinical studies in humans have shown that the extracellular concentration of glutamate increases to neurotoxic levels in ischemia (Kostandy, 2012; Lai et al., 2014; Nishizawa, 2001). Glutamate is believed to contribute to neuronal damage in humans suffering from acute degenerative disorders such as stroke (Chan et al., 1986; Chao et al., 2010). Glutamate stimulation of α-amino-3-hydroxy-5-methyl-4-isoxazolone-proprionic acid (AMPA) receptors increases sodium uptake by neurons, contributing to cellular edema. However, glutamatergic stimulation of N-methyl-D-aspartate (NMDA) receptors by glutamate increases intracellular calcium concentrations and cell death (Weinberger, 2006). Despite the extensive and continued research focusing on the mechanisms of excitotoxicity, there are currently no pharmacological interventions capable of providing significant neuroprotection in patients suffering from brain ischemia or injury (Puyal et al., 2013). Although the results in human trials have not been positive, they have advanced the understanding of neuroprotection in ischemic stroke treatment and revealed better strategies for conducting clinical trials in this area (Weinberger, 2006). In this sense, efforts have been made to reduce glutamate levels during earlier stages of excitotoxicity by inhibiting synthesis or release. Thus, compounds that block the uptake of glutamate into synaptic vesicles may reduce excitotoxic events (Thompson et al., 2005). In this work we have observed that JM-20 inhibited glutamate uptake by synaptic vesicles in association with an inhibition of V-ATPase activity and a dissipation of ΔpH. These related effects may contribute to the reduction of glutamate quantal size, thus reducing the glutamate released into the synapses, and could partly explain the anti-excitotoxic effect we recently observed *in vivo* (Nuñez-Figueredo et al., 2014b).

An apparent divergent effect of JM-20 on glutamate release in synaptosomes (inhibition) and the cell culture (no effect) was observed. Unlike primary cell culture, synaptosomal fraction from whole brain is not homogeneous. Indeed, different populations of synaptic-like vesicles from rat brain with marked biochemical heterogeneity have been described (Provoda et al., 2000; Thoidis et al., 1998). Thus the dissimilar effects of JM-20 on primary culture of cortical neurons and synaptosomes suggest that the observed pharmacological effects of this molecule are related not only to its action toward a specific neuronal cell type, but also to a more complex mechanism involving different components of the neurovascular unit.

We also observed that JM-20 inhibited glutamate release in a more complex brain synaptosome system, which represents an excellent model to study the effects of substances with potential activity in the central nervous system. Because this effect was observed during K^+-evoked glutamate release, it could result from different mechanisms of action of this molecule: (*i*) it is inhibiting the Na^+-dependent glutamate transporters (EAATs) located on the plasma membrane of neurons and glial cells, or (*ii*) it does not affect such transporters but is instead diminishing the amount of glutamate released by the vesicular-mediated effects described above. The latter mechanism may increase the cytosolic levels of glutamate, which in turn may downregulate the transmitter release and also its uptake. It is worth noticing that non vesicular glutamate accumulation (i.e. cytosolic) may contribute to elevate extracellular glutamate concentration through cystine/glutamate antiporter (Soria et al., 2014). In this sense, it would appear that the vesicular glutamate transport inhibition by JM-20 would further aggravate the excitotoxicity, rather than protect it. It has been observed that the increased spontaneous vesicular transmitter release caused by energy depletion or bafilomycin A1 only leads to extracellular glutamate accumulation when glial glutamate uptake is blocked (Gebhardt et al., 2002; Jabaudon et al., 2000; Soria et al., 2014). We observed here that JM-20 enhanced glutamate uptake in astrocyte culture alone at very low micromolar concentrations, but it did not, in cortical neurons. Because the astrocytic glutamate transport plays a major role in maintaining extracellular glutamate concentrations below neurotoxic levels (Anderson and Swanson, 2000; Danbolt, 2001), and the neurotransmitter uptake by astrocytes can be stimulated by several neuroprotective compounds (Beller et al., 2011; Karki et al., 2014; Wu et al., 2008), the above mentioned effects of JM-20 may contribute to explain its anti-excitotoxic actions *in vitro* (Nuñez-Figueredo et al., 2014a) and *in vivo* (Nuñez-Figueredo et al., 2014b).

Astrocytes actively shape the dynamics of neurons and neuronal ensembles by affecting several aspects critical to neuronal function, such as regulating synaptic plasticity, modulating neuronal excitability, and maintaining extracellular ion balance (Volman et al., 2012). Thus, there is an active and bi-directional interaction

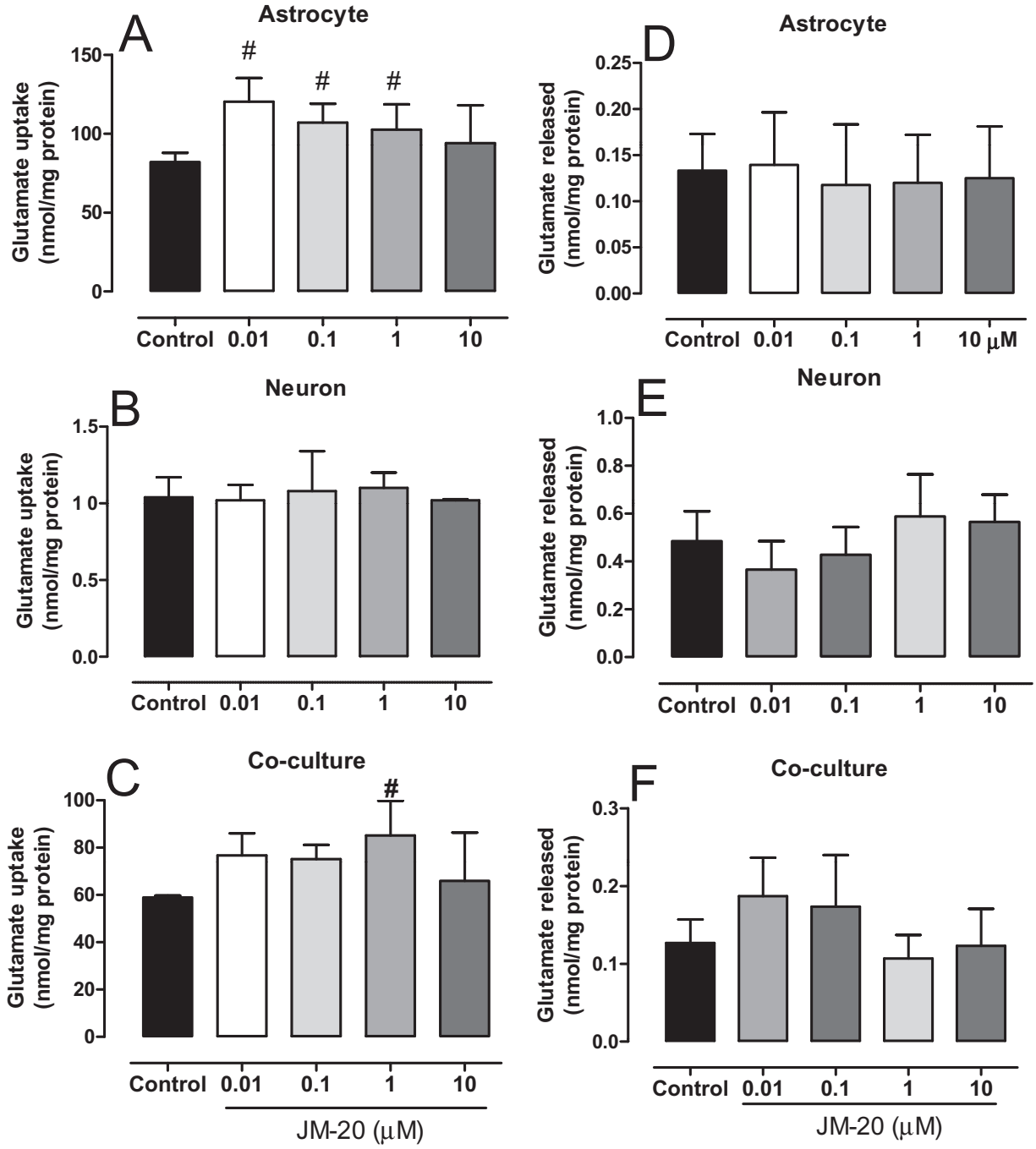

Fig. 4. Effect of JM-20 (1 and 10 μM) on glutamate uptake (A–C) or glutamate release (D–F) by astrocytes (A, D), neurons (B, E) and astrocyte–neuron co-cultures (C, F). Cell cultures (astrocytes, neurons and co-culture) were incubated for 15 min with HBSS pH 7.4. Glutamate uptake was carried out at 35 °C by adding 100 μM unlabeled glutamate and 0.33 μCi/ml L-[^{3}H] glutamate for 5 min. JM-20 (0.01, 0.1, 1, and 10 μM) or DMSO (Control, 1/1000 dilution) was added 20 min before to L-[^{3}H] glutamate. Sodium-dependent uptake was obtained by subtracting sodium-independent uptake from total uptake. Data are means ± S.E.M., n = 6. Statistically significant differences from controls are represented by $^{\#}p < 0.05$ according to ANOVA and *post hoc* Newman–Keuls tests.

between glia and neurons that challenges any *in vitro* results obtained with neurons or astrocytes in culture alone. In this sense, we observed that like in astrocytes, JM-20 increased glutamate uptake in cortical neurons/astrocytes co-culture. This suggests that hitherto unidentified astrocyte-derived factors may be responsible for the JM-20 effects, either by eliciting direct neuroprotective effects or by modulating the microglial response to neuronal injury.

In summary, JM-20 seems to exert a modulatory action on the glutamatergic system by inhibiting the vesicular ATPase activity, which in turn prevents the establishment of the electrochemical proton gradient across the vesicular membrane, with a marked inhibition of glutamate uptake. JM-20 also inhibited glutamate release in synaptosomal membranes. Additionally, JM-20 increased glutamate uptake in astrocyte culture alone or co-cultured with neurons, an effect probably mediated by the glial cells signals. These actions may contribute to the maintenance of extracellular glutamate concentrations below neurotoxic levels. Finally, these results provide further evidence of the neuroprotective potential of JM-20 in pathologies that involve excessive glutamate release, such as cerebral ischemia, and contribute to the explanation of the anti-excitotoxic

effect of JM-20 observed *in vivo* (Nuñez-Figueredo et al., 2014b). Unfortunately, even though animal models demonstrate dramatic histological and behavioral neuroprotection with JM-20 (Nuñez-Figueredo et al., 2014b), no pharmacological intervention with drugs that affect glutamatergic transmission has yet been shown to provide benefit in humans, and toxicity remains a large obstacle (Lau and Tymianski, 2010; Muir, 2006). Thus, the clinical usefulness of JM-20 will also depend on its acute and chronic side effects. Indeed, because the filling of synaptic vesicles with monoamines also depends on the energy stored in a H^+ electrochemical gradient produced by the vacuolar-type H^+-ATPase (Hnasko and Edwards, 2012), JM-20 could interfere with monoaminergic transmission by affecting monoamines vesicular loading as well. Increased cytosolic accumulation due to the perturbation of catecholamine accumulation into storage vesicles could cause increased oxidative stress and oxidative damage to the catecholaminergic neurons (Adams et al., 2001; Liu and Edwards, 1997). Thus, the potential neurotoxic and addictive effects of JM-20 related to its potential impairment of monoaminergic transmission need to be addressed.

Acknowledgments

This work was partially supported by CAPES-Brazil/MES-Cuba projects 140/11 and 092/10, INCT-EN/CNPq (Brazil), IBN.Net/CNPq (Brazil), FAPERGS/RS, and the Non-Governmental Organization MEDICUBA-SPAIN.

References

Adams, J.D., Jr., Chang, M.L., Klaidman, L., 2001. Parkinson's disease–redox mechanisms. Curr. Med. Chem. 8, 809–814.
Anderson, C.M., Swanson, R.A., 2000. Astrocyte glutamate transport: guanosine and GMP prevent seizures induced by quinolinic acid in review of properties, regulation, and physiological functions. Glia 32, 1–14.
Beller, J.A., Gurkoff, G.G., Berman, R.F., Lyeth, B.G., 2011. Pharmacological enhancement of glutamate transport reduces excitotoxicity in vitro. Restor. Neurol. Neurosci. 29, 331–346.
Chan, K.M., Delfert, D., Junger, K.D., 1986. A direct colorimetric assay for Ca^{2+}-stimulated ATPase activity. Anal. Biochem. 157, 375–380.
Chao, X.D., Fei, F., Fei, Z., 2010. The role of excitatory amino acid transporters in cerebral ischemia. Neurochem. Res. 35, 1224–1230.
Danbolt, N.C., 2001. Glutamate uptake. Prog. Neurobiol. 65, 1–105.
Dienel, G.A., Hertz, L., 2005. Astrocytic contributions to bioenergetics of cerebral ischemia. Glia 50, 362–388.
Figueredo, Y.N., Rodriguez, E.O., Reyes, Y.V., Dominguez, C.C., Parra, A.L., Sanchez, J.R., , 2013. Characterization of the anxiolytic and sedative profile of JM-20: a novel benzodiazepine-dihydropyridine hybrid molecule. Neurol. Res. 35, 804–812.
Frizzo, M.E., Lara, D.R., Dahm, K.C., Prokopiuk, A.S., Swanson, R.A., Souza, D.O., 2001. Activation of glutamate uptake by guanosine in primary astrocyte cultures. Neuroreport 12, 879–881.
Gebhardt, C., Körner, R., Heinemann, U., 2002. Delayed anoxic depolarizations in hippocampal neurons of mice lacking the excitatory amino acid carrier 1. J. Cereb. Blood Flow Metab. 22, 569–575.
Godino, M., Torres, M., Sánchez-Prieto, J., 2007. CB1 receptors diminish both Ca(2+) influx and glutamate release through two different mechanisms active in distinct populations of cerebrocortical nerve terminals. J. Neurochem. 101, 1471–1482.
Goh, G.Y., Huang, H., Ullman, J., Borre, L., Hnasko, T.S., Trussell, L.O., et al., 2011. Presynaptic regulation of quantal size: K^+/H^+ exchange stimulates vesicular glutamate transport. Nat. Neurosci. 14, 1285–1292.
Hnasko, T.S., Edwards, R.H., 2012. Neurotransmitter corelease: mechanism and physiological role. Annu. Rev. Physiol. 74, 225–243.
Jabaudon, D., Scanziani, M., Gähwiler, B.H., Gerber, U., 2000. Acute decrease in net glutamate uptake during energy deprivation. Proc. Natl. Acad. Sci. U.S.A. 97, 5610–5615.
Joseph, M.H., Marsden, C.A., 1986. Amino acids and small peptides. In: Lim, C.K. (Ed.), HPLC of Small Molecules; a Practical Approach. IRL Press, Oxford, pp. 13–47.
Juge, N., Gray, J.A., Omote, H., Miyaji, T., Inoue, T., Hara, C., et al., 2010. Metabolic control of vesicular glutamate transport and release. Neuron 68, 99–112.
Karki, P., Webb, A., Zerguine, A., Choi, J., Son, D.S., Lee, E., 2014. Mechanism of raloxifene-induced upregulation of glutamate transporters in rat primary astrocytes. Glia 62, 1270–1283.
Kostandy, B.B., 2012. The role of glutamate in neuronal ischemic injury: the role of spark in fire. Neurol. Sci. 33, 223–237.
Lai, T.W., Zhang, S., Wang, Y.T., 2014. Excitotoxicity and stroke: identifying novel targets for neuroprotection. Prog. Neurobiol. 115, 157–188.
Lau, A., Tymianski, M., 2010. Glutamate receptors, neurotoxicity and neurodegeneration. Pflugers Arch. 460, 525–542.
Lin, R.C., Scheller, R.H., 2000. Mechanisms of synaptic vesicle exocytosis. Annu. Rev. Cell Dev. Biol. 16, 19–49.
Liu, Y., Edwards, R.H., 1997. The role of vesicular transport proteins in synaptic transmission and neural degeneration. Annu. Ver. Neurosci. 20, 125–156.
Loureiro, S.O., Romão, L., Alves, T., Fonseca, A., Heimfarth, L., Moura Neto, V., et al., 2010. Homocysteine induces cytoskeletal remodeling and production of reactive oxygen species in cultured cortical astrocytes. Brain Res. 1355, 151–164.
Lowry, O.H., Rosebrough, N.J., Farr, A.L., Randall, R.J., 1951. Protein measurement with the folin phenol reagent. J. Biol. Chem. 193, 265–275.
Maycox, P.R., Deckwerth, T., Hell, J.W., Jahn, R., 1988. Glutamate uptake by brain synaptic vesicles. Energy dependence of transport and functional reconstitution in proteoliposomes. J. Biol. Chem. 263, 15423–15428.
Mehta, A., Prabhakar, M., Kumar, P., Deshmukh, R., Sharma, P.L., 2013. Excitotoxicity: bridge to various triggers in neurodegenerative disorders. Eur. J. Pharmacol. 698, 6–18.
Moura Neto, V., Mallat, M., Jeantet, C., Prochiantz, A., 1983. Microheterogeneity of tubulin proteins in neuronal and glial cells from the mouse brain in culture. EMBO J. 2, 1243–1248.
Muir, K.W., 2006. Glutamate-based therapeutic approaches: clinical trials with NMDA antagonists. Curr. Opin. Pharmacol. 6, 53–60.
Naito, S., Ueda, T., 1985. Characterization of glutamate uptake into synaptic vesicles. J. Neurochem. 44, 99–109.
Nelson, N., Harvey, W.R., 1999. Vacuolar and plasma membrane proton-adenosine triphosphatases. Physiol. Rev. 79, 361–385.
Nishizawa, Y., 2001. Glutamate release and neuronal damage in ischemia. Life Sci. 69, 369–381.
Nuñez-Figueredo, Y., Ramírez-Sánchez, J., Delgado-Hernández, R., Porto-Verdecia, M., Ochoa-Rodríguez, E., Verdecia-Reyes, Y., et al., 2014a. JM-20, a novel benzodiazepine–dihydropyridine hybrid molecule, protects mitochondria and prevents ischemic insult-mediated neural cell death in vitro. Eur. J. Pharmacol. 726, 57–65.
Nuñez-Figueredo, Y., Ramírez-Sánchez, J., Hansel, G., Nicoloso-Simões, E., Merino, N., Valdes, O., et al., 2014b. A novel multi-target ligand (JM-20) protects mitochondrial integrity, inhibits brain excitatory amino acids release and reduces cerebral ischemia injury in vitro and in vivo. Neuropharmacology 85, 517–527.
Porciuncula, L.O., Rocha, J.B., Tavares, R.G., Ghisleni, G., Reis, M., Souza, D.O., 2003. Methylmercury inhibits glutamate uptake by synaptic vesicles from rat brain. Neuroreport 14, 577–580.
Provoda, C.J., Waring, M.T., Buckley, K.M., 2000. Evidence for a primary endocytic vesicle involved in synaptic vesicle biogenesis. J. Biol. Chem. 275, 7004–7012.
Puyal, J., Ginet, V., Clarke, P.G., 2013. Multiple interacting cell death mechanisms in the mediation of excitotoxicity and ischemic brain damage: a challenge for neuroprotection. Prog. Neurobiol. 105, 24–48.
Schmidt, A.P., Tort, A.B., Silveira, P.P., Bohmer, A.E., Hansel, G., Knorr, L., et al., 2009. The NMDA antagonist MK-801 induces hyperalgesia and increases CSF excitatory amino acids in rats: reversal by guanosine. Pharmacol. Biochem. Behav. 91, 549–553.
Sims, N.R., 1990. Rapid isolation of metabolically active mitochondria from rat brain and subregions using percoll density gradient centrifugation. J. Neurochem. 55, 698–707.
Soria, F.N., Pérez-Samartín, A., Martin, A., Gona, K.B., Llop, J., Szczupak, B., et al., 2014. Extrasynaptic glutamate release through cystine/glutamate antiporter contributes to ischemic damage. J. Clin. Invest. 124, 3645–3655.
Thoidis, G., Chen, P., Pushkin, A.V., Vallega, G., Leeman, S.E., Fine, R.E., et al., 1998. Two distinct populations of synaptic-like vesicles from rat brain. Proc. Natl. Acad. Sci. U.S.A. 95, 183–188.
Thompson, C.M., Davis, E., Carrigan, C.N., Cox, H.D., Bridges, R.J., Gerdes, J.M., 2005. Inhibitor of the glutamate vesicular transporter (VGLUT). Curr. Med. Chem. 12, 2041–2056.
Uyemura, S.A., Curti, C., 1992. Steady-state kinetic properties of FoF1-atpase: the pH effect. Int. J. Biochem. 24, 1743–1748.
Volman, V., Bazhenov, M., Sejnowski, T.J., 2012. Computational models of neuron-astrocyte interaction in epilepsy. Front. Comput. Neurosci. 6, 58.
Weinberger, J.M., 2006. Evolving therapeutic approaches to treating acute ischemic stroke. J. Neurol. Sci. 249, 101–109.
Wu, J.Y., Niu, F.N., Huang, R., Xu, Y., 2008. Enhancement of glutamate uptake in 1-methyl-4-phenylpyridinium-treated astrocytes by trichostatin A. Neuroreport 19, 1209–1212.